# Temperature- and Structural-Dependent Optical Properties and Photophysics of BODIPY Dyes

*Sebastian Radunz,[a] Werner Kraus,[a] Florian A. Bischoff,[b] Franziska Emmerling,[a,b] Harald Rune Tschiche[c] and Ute Resch-Genger*[a]*

*[a] Department 1 – Analytical Chemistry; Reference Materials, Federal Institute for Materials Research and Testing (BAM), Richard-Willstaetter-Str. 11, 12489 Berlin, Germany. E-mail: ute.resch@bam.de*
*[b] Department of Chemistry, Humboldt-Universität zu Berlin, Brook-Taylor-Straße 2, 12489 Berlin, Germany.*
*[c] Department of Chemical and Product Safety, German Federal Institute for Risk Assessment (BfR), Max-Dohrn-Str. 8-10, 10589 Berlin, Germany.*

*Electronic Supplementary Information (ESI)*

## Experimental Section

**Synthesis of fluorescent pH sensitive BODIPYs:**
The corresponding aldehyde (2.5 mmol, 1.0 eq.) and 2,4-dimethylpyrrole (5.0 mmol, 2.0 eq.) were dissolved in 140 ml dry DCM and 10 ml dry EtOH. After degassing by rapid vacuum-argon cycles (5 times), a few drops of TFA (30 µl) were added and the reaction mixture was stirred at room temperature under argon atmosphere in the dark overnight. *p*-Chloranil (2.5 mmol, 1.0 eq.) was added and the mixture was stirred for additional 60 min. Prior addition of $BF_3 \cdot OEt_2$ (25.0 mmol, 10.0 eq.) and 4.3 ml diisopropylethylamine (DIPEA) (25.0 mmol, 10.0 eq.), the DCM/EtOH solvent mixture was removed under reduced pressure and replaced by 100 ml of dry DCM to avoid a reaction between $BF_3 \cdot OEt_2$ and EtOH. After portionwise addition, the reaction mixture was stirred for 60 minutes. Subsequently, the reaction mixture was prepurified by carrying out a short silica-gel flash column chromatography with DCM as eluent. The resulting crude mixture was concentrated under reduced pressure and further purified by

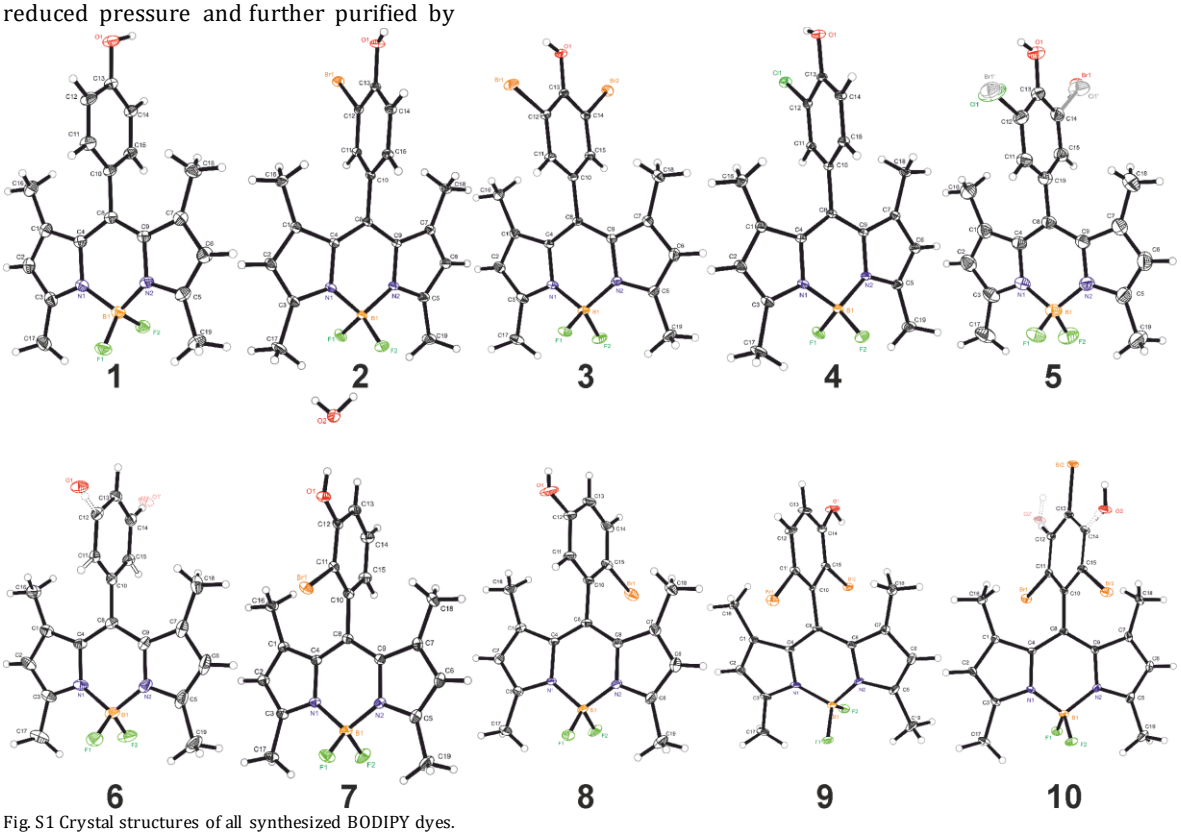

Fig. S1 Crystal structures of all synthesized BODIPY dyes.

**Table S1.** Selected crystallographic data and structure refinement parameters.

| Compound reference | 1 | 2 | 3 | 4 | 5 | 6 | 7 | 8 | 9 | 10 |
|---|---|---|---|---|---|---|---|---|---|---|
| Chemical formula | $C_{19}H_{19}BF_2N_2O$ | $C_{19}H_{18}BBrF_2N_2O$ | $C_{19}H_{17}BBr_2FN_2O$ | $C_{19}H_{18}BClF_2N_2O$ | $C_{19}H_{17}BBrClF_2N_2O$ | $C_{19}H_{18}BF_2N_2O$ | $C_{19}H_{20}BBrF_2N_2O_2$ | $C_{19}H_{18}BBrF_2N_2O$ | $C_{19}H_{17}BBr_2F_2N_2O$ | $C_{19}H_{16}BBr_3F_2N_2O$ |
| Formula Mass /g mol$^{-1}$ | 340.17 | 419.07 | 497.97 | 374.61 | 452.51 | 339.16 | 437.09 | 419.07 | 497.97 | 576.88 |
| Crystal system | monoclinic | monoclinic | monoclinic | monoclinic | monoclinic | monoclinic | monoclinic | monoclinic | monoclinic | monoclinic |
| $a$ /Å | 13.8943 | 16.0546 | 12.6348 | 15.8689 | 12.6330 | 13.8906 | 11.4965 | 7.0391 | 13.4725 | 26.5236 |
| $b$/Å | 9.6155 | 13.4873 | 10.6680 | 13.4387 | 10.7186 | 25.8723 | 8.9786 | 14.1435 | 19.8851 | 10.3333 |
| $c$/Å | 13.8974 | 16.4137 | 15.1098 | 16.2719 | 15.1341 | 14.1900 | 18.2352 | 20.8508 | 7.4708 | 17.5893 |
| $\alpha$/° | 90 | 90 | 90 | 90 | 90 | 90 | 90 | 90 | 90 | 90 |
| $\beta$/° | 113.810 | 96.9234 | 107.3285 | 95.8495 | 107.1048 | 91.0486 | 91.431 | 91.1289 | 109.6622 | 125.3134 |
| $\gamma$/° | 90 | 90 | 90 | 90 | 90 | 90 | 90 | 90 | 90 | 90 |
| Unit cell volume /Å$^3$ | 1698.7 | 3528.2 | 1944.18 | 3452.0 | 1958.64 | 5098.8 | 1881.68 | 2075.45 | 1884.74 | 3933.8 |
| Temperature /K | 150(2) | 150(2) | 150(2) | 150(2) | 297(2) | 150(2) | 150(2) | 150(2) | 150(2) | 150(2) |
| Space group | *P*21/*n* | *P*21/*n* | *P*21/*n* | *P*21/*n* | *P*21/*n* | *P*21/*c* | *Cc* | *P*21/*n* | *Cc* | *C*2/*c* |
| No. of formula units per unit cell, $Z$ | 4 | 8 | 4 | 8 | 4 | 12 | 4 | 4 | 4 | 8 |
| Absorption coefficient, $\mu$/mm$^{-1}$ | 0.097 | 2.361 | 4.199 | 0.252 | 2.264 | 0.097 | 2.220 | 2.007 | 4.332 | 6.184 |
| No. of reflections measured | 29038 | 107330 | 74846 | 92931 | 42661 | 130154 | 27890 | 67769 | 30356 | 101847 |
| No. of independent reflections | 4224 | 10821 | 9966 | 11048 | 4887 | 12704 | 4698 | 6364 | 6201 | 13128 |
| $R_{int}$ | 0.1955 | 0.0933 | 0.1082 | 0.1039 | 0.1257 | 0.1993 | 0.0936 | 0.1050 | 0.1371 | 0.0817 |
| Final $R_1$ values ($I > 2\sigma(I)$) | 0.0736 | 0.0407 | 0.0459 | 0.0628 | 0.0440 | 0.1276 | 0.0335 | 0.0569 | 0.0546 | 0.0628 |
| Final $wR(F^2)$ values ($I > 2\sigma(I)$) | 0.1696 | 0.0986 | 0.1120 | 0.1494 | 0.1111 | 0.2203 | 0.0852 | 0.1203 | 0.1181 | 0.1156 |
| Final $R_1$ values (all data) | 0.1274 | 0.0520 | 0.0739 | 0.0878 | 0.0654 | 0.1943 | 0.0342 | 0.0719 | 0.0775 | 0.1054 |
| Final $wR(F^2)$ values (all data) | 0.1989 | 0.1060 | 0.1252 | 0.1640 | 0.1268 | 0.2431 | 0.0859 | 0.1272 | 0.1455 | 0.1287 |
| Goodness of fit on $F^2$ | 1.034 | 1.022 | 1.013 | 1.051 | 1.074 | 1.222 | 1.044 | 1.085 | 1.071 | 1.084 |
| CCDC number | 1969036 | 1969037 | 1969038 | 1969039 | 1969040 | 1969041 | 1969042 | 1969043 | 1969044 | 1969045 |

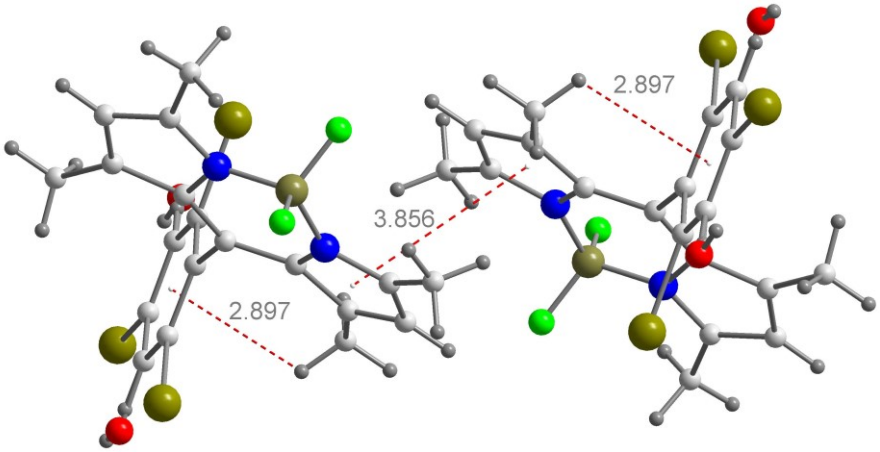


*Fig. S2 Crystal packing and stabilizing inter- and intramolecular interactions.*

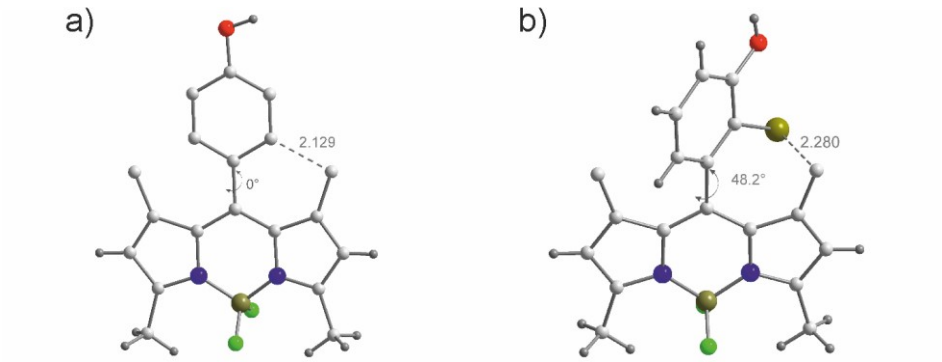


*Fig. S3 Hypothetical rotation of the meso-aryl along the C8-C10 axis of BODIPY **1** and **7**.*

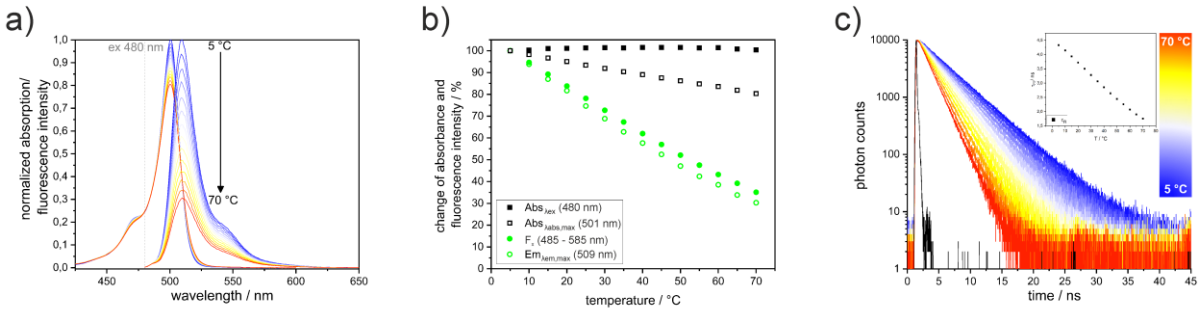


Fig. S4 a) Temperature-dependent normalized absorption and normalized fluorescence intensity of non-sterically hindered compound **2** upon excitation at 480 nm. b) Percentage changes of the absorbance (black squares) at excitation wavelength and at maximum absorbance (full and open symbols, respectively), and percentage changes of the fluorescence intensity (green circles) for integrated emission intensity and at emission maximum (full and open symbols, respectively) in dependence of temperature for compound **2**. c) Fluorescence decay curves for compound **2** in dependence of the temperature (black line represents the instrument response function (IRF)). The inset shows the mono exponential fitted fluor escence lifetime as function of temperature.

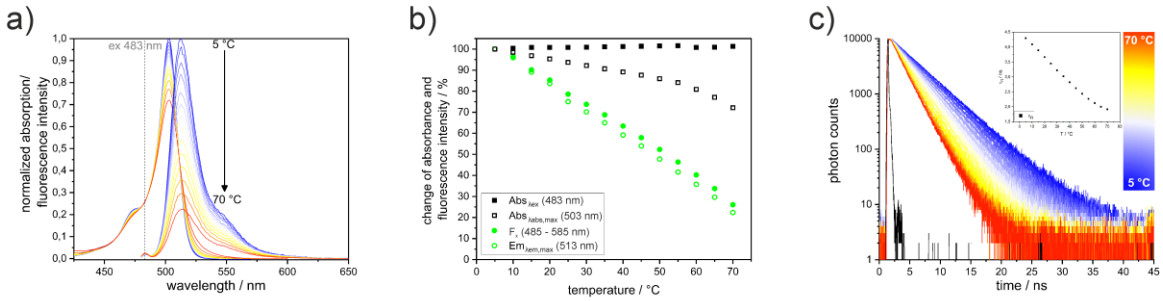


Fig. S5 a) Temperature-dependent normalized absorption and normalized fluorescence intensity of non-sterically hindered compound **3** upon excitation at 483 nm. b) Percentage changes of the absorbance (black squares) at excitation wavelength and at maximum absorbance (full and open symbols, respectively), and percentage changes of the fluorescence intensity (green circles) for integrated emission intensity and at emission maximum (full and open symbols, respectively) in dependence of temperature for compound **3**. c) Fluorescence decay curves for compound **3** in dependence of the temperature (black line represents the instrument response function (IRF)). The inset shows the mono exponential fitted fluor escence lifetime as function of temperature.

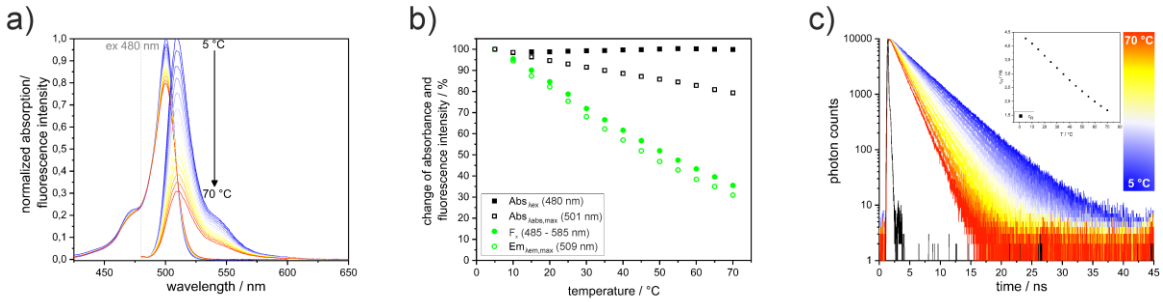


Fig. S6 a) Temperature-dependent normalized absorption and normalized fluorescence intensity of non-sterically hindered compound **4** upon excitation at 480 nm. b) Percentage changes of the absorbance (black squares) at excitation wavelength and at maximum absorbance (full and open symbols, respectively), and percentage changes of the fluorescence intensity (green circles) for integrated emission intensity and at emission maximum (full and open symbols, respectively) in dependence of temperature for compound **4**. c) Fluorescence decay curves for compound **4** in dependence of the temperature (black line represents the instrument response function (IRF)). The inset shows the mono exponential fitted fluorescence lifetime as function of temperature.

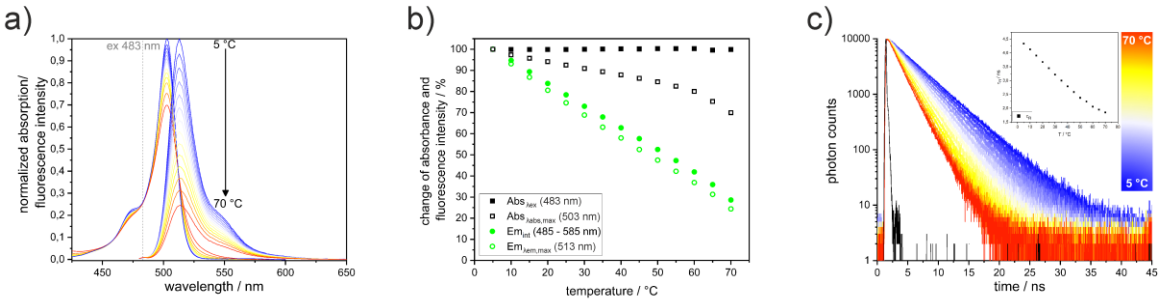


Fig. S7 a) Temperature-dependent normalized absorption and normalized fluorescence intensity of non-sterically hindered compound **5** upon excitation at 483 nm. b) Percentage changes of the absorbance (black squares) at excitation wavelength and at maximum absorbance (full and open symbols, respectively), and percentage changes of the fluorescence intensity (green circles) for integrated emission intensity and at emission maximum (full and open symbols, respectively) in dependence of temperature for compound **5**. c) Fluorescence decay curves for compound **5** in dependence of the temperature (black line represents the instrument response function (IRF)). The inset shows the mono exponential fitted fluorescence lifetime as function of temperature.

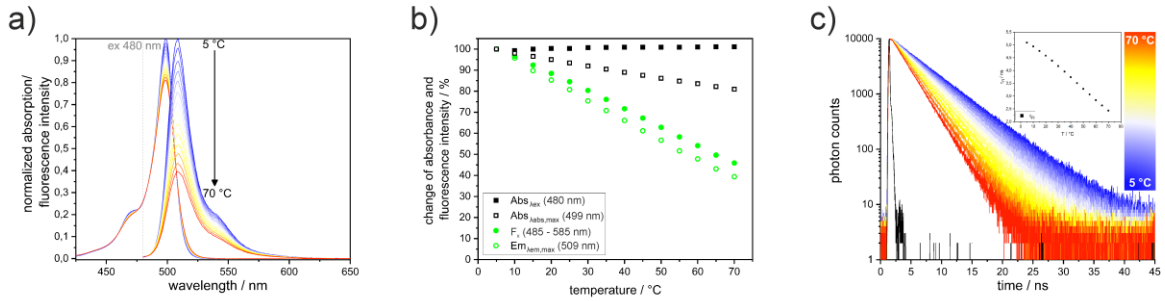


Fig. S8 a) Temperature-dependent normalized absorption and normalized fluorescence intensity of non-sterically hindered compound **6** upon excitation at 480 nm. b) Percentage changes of the absorbance (black squares) at excitation wavelength and at maximum absorbance (full and open symbols, respectively), and percentage changes of the fluorescence intensity (green circles) for integrated emission intensity and at emission maximum (full and open symbols, respectively) in dependence of temperature for compound **6**. c) Fluorescence decay curves for compound **6** in dependence of the temperature (black line represents the instrument response function (IRF)). The inset shows the mono exponential fitted fluorescence lifetime as function of temperature.

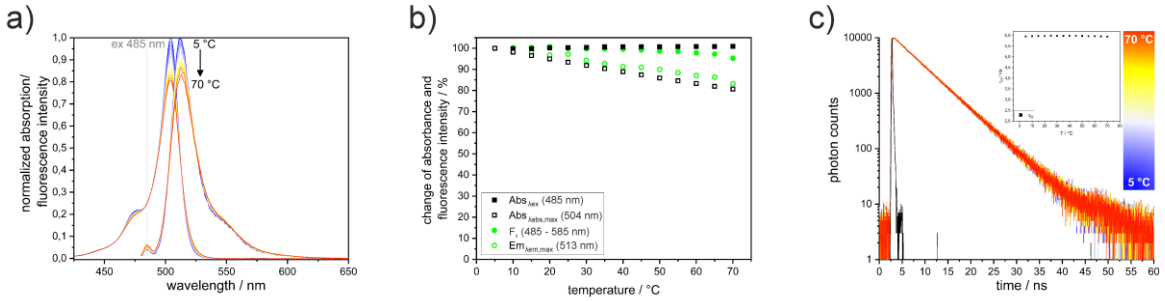


Fig. S9 a) Temperature-dependent normalized absorption and normalized fluorescence intensity of sterically hindered compound **8** upon excitation at 485 nm. b) Percentage changes of the absorbance (black squares) at excitation wavelength and at maximum absorbance (full and open symbols, respectively), and percentage changes of the fluorescence intensity (green circles) for integrated emission intensity and at emission maximum (full and open symbols, respectively) in dependence of temperature for compound **8**. c) Fluorescence decay curves for compound **8** in dependence of the temperature (black line represents the instrument response function (IRF)). The inset shows the mono exponential fitted fluorescence lifetime as function of temperature.

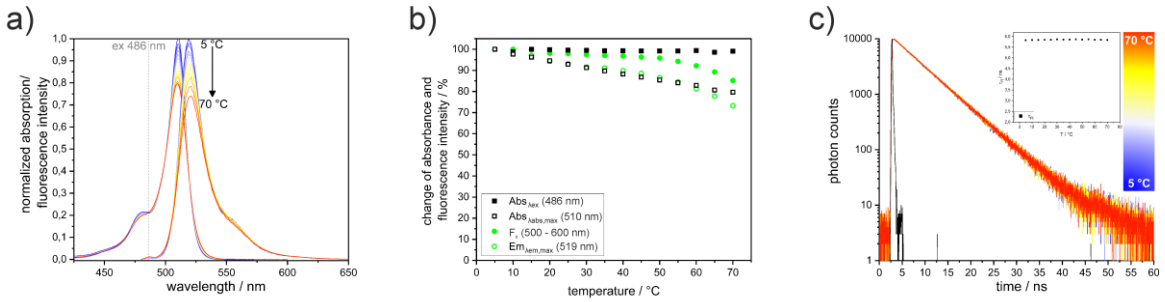


Fig. S10 a) Temperature-dependent normalized absorption and normalized fluorescence intensity of sterically hindered compound **9** upon excitation at 486 nm. b) Percentage changes of the absorbance (black squares) at excitation wavelength and at maximum absorbance (full and open symbols, respectively), and percentage changes of the fluorescence intensity (green circles) for integrated emission intensity and at emission maximum (full and open symbols, respectively) in dependence of temperature for compound **9**. c) Fluorescence decay curves for compound **9** in dependence of the temperature (black line represents the instrument response function (IRF)). The inset shows the mono exponential fitted fluorescence lifetime as function of temperature.

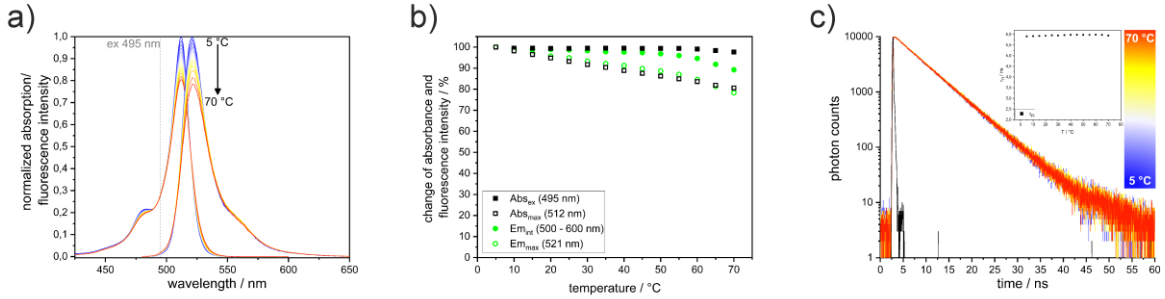


Fig. S11 a) Temperature-dependent normalized absorption and normalized fluorescence intensity of sterically hindered compound **10** upon excitation at 495 nm. b) Percentage changes of the absorbance (black squares) at excitation wavelength and at maximum absorbance (full and open symbols, respectively), and percentage changes of the fluorescence intensity (green circles) for integrated emission intensity and at emission maximum (full and open symbols, respectively) in dependence of temperature for compound **10**. c) Fluorescence decay curves for compound **10** in dependence of the temperature (black line represents the instrument response function (IRF)). The inset shows the mono exponential fitted fluorescence lifetime as function of temperature.

**Table S2.** Calculated absolute and relative energies of the minimum (min1, min2), the transition (TS1, TS2) and intermediate (IS) states and corresponding dihedral angles of BODIPY compounds **1**, **3**, **6**, **7**, **8** and **9**.

| Dye | *absolute energy / $E_h$ (relative energy / kcalmol$^{-1}$)* | | | | | *dihedral angle[a] / °* | | | | | $t_{1/2}$[b] / *s (20 °C)* |
|---|---|---|---|---|---|---|---|---|---|---|---|
| | min 1 | TS 1 | IS | TS 2 | min 2 | min 1 | TS 1 | IS | TS 2 | min 2 | *min->TS1* |
| **1** | 0 | 16.4 | 16.1 | 16.4 | 0 | 90 | 14 | 3 | -14 | -90 | 0.2 |
| **3** | 0 | 16.7 | - | - | 0.03 | 90 | 14 | | | -93 | 0.3 |
| **6** | 0 | 12.9 | 12.7 | 12.8 | 0 | 40 | 13 | 3 | -13 | -40 | $4.8 * 10^{-4}$ |
| **7** | 0 | 42.3 | - | - | 0 | | 34 | | | | $3.9 * 10^{18}$ |
| **8** | 0 | 38.2 | - | - | 0.3 | 89 | 29 | | | -92 | $3.1 * 10^{15}$ |
| **9** | 0 | 49.2 | 46.6 | 49.2 | 0 | 90 | 39 | 10.5 | -39 | -90 | $5.1 * 10^{23}$ |

[a] Dihedral angle determined by....

[b] Half-life calculated assuming first order reaction kinetics $t_{1/2} = \frac{\ln(2)}{k}$, with $k = \kappa \frac{k_B T}{h} e^{-\frac{\Delta G}{RT}}$ from Eyring equation with $k_B$ = Boltzmann constant, T = 293.15 K, h = Planck constant, κ = 1 (transmission coefficient) and R = gas constant.

**Table S3.** Temperature-dependent non-radiative decay rates $k_{nr}$.

| Dye | $k_{nr}$ (T) / $10^8$ s$^{-1}$ | | |
|---|---|---|---|
| | 5 °C | 20 °C | 70 °C |
| **1** | 0.66 ± 0.05 | 1.16 ± 0.05 | 4.91 ± 0.05 |
| **2** | 0.62 ± 0.06 | 1.07 ± 0.06 | 4.29 ± 0.06 |
| **3** | 0.72 ± 0.05 | 1.15 ± 0.05 | 4.32 ± 0.05 |
| **4** | 0.71 ± 0.07 | 1.12 ± 0.07 | 4.53 ± 0.07 |
| **5** | 0.71 ± 0.05 | 1.15 ± 0.05 | 4.36 ± 0.05 |
| **6** | 0.29 ± 0.02 | 0.55 ± 0.02 | 2.57 ± 0.02 |
| **7** | 0.15 ± 0.01 | 0.15 ± 0.01 | 0.24 ± 0.01 |
| **8** | 0.18 ± 0.01 | 0.18 ± 0.01 | 0.30 ± 0.01 |
| **9** | 0.18 ± 0.01 | 0.21 ± 0.01 | 0.43 ± 0.01 |
| **10** | 0.20 ± 0.01 | 0.22 ± 0.01 | 0.37 ± 0.01 |

**Table S4.**.Fitting parameters fot the determination of $\Delta E_A$ for non-radiative decay of the first exited state $S_1$

| Dye | $\frac{\Delta E_A}{R}$ ($\Phi_{Fl}$) / K[a] | $E_A(\Phi_{Fl})$ / kcalmol$^{-1}$[a] | ln (c2) ($\Phi_{Fl}$)[a] | $R^2$ ($\Phi_{Fl}$) | $\frac{\Delta E_A}{R}$ ($\tau_{Fl}$) / K[b] | $E_A(\tau_{Fl})$ / kcalmol$^{-1}$[b] | ln (A) ($\tau_{Fl}$) | $c_3$ ($\tau_{Fl}$)/ $10^8$ $s^{-1}$* | $R^2$ ($\tau_{Fl}$) |
|---|---|---|---|---|---|---|---|---|---|
| **1** | -3030 ± 19 | 6.02 ± 0.30 | 9,97 ± 0,06 | 0,999 | -2981 ± 13 | 5.92 ± 0.30 | 7,94 ± 0,04 | 1,75 | 0,999 |
| **2** | -3058 ± 12 | 6.08 ± 0.30 | 10,00 ± 0,04 | 0,999 | -2956 ± 11 | 5.87 ± 0.29 | 7,68 ± 0,03 | 1,78 | 0,999 |
| **3** | -3255 ± 133 | 6.47 ± 0.32 | 10,79 ± 0,43 | 0,979 | -3029 ± 10 | 6.02 ± 0.22 | 7,94 ± 0,03 | 1,78 | 0,999 |
| **4** | -2972 ± 30 | 5.91 ± 0.30 | 9,80 ± 0,10 | 0,999 | -2989 ± 19 | 5.94 ± 0.30 | 7,84 ± 0,06 | 1,79 | 0,999 |
| **5** | -3101 ± 100 | 6.16 ± 0.31 | 10,26 ± 0,32 | 0,987 | -3046 ± 7 | 6.05 ± 0.23 | 8,02 ± 0,02 | 1,78 | 0,998 |
| **6** | -3289 ± 32 | 6.54 ± 0.33 | 10,11 ± 0,11 | 0,999 | -3241 ± 28 | 6.44 ± 0.32 | 8,02 ± 0,09 | 1,70 | 0,999 |
| **7** | -739 ± 56 | 1.47 ± 0.29 | 0,21± 0,18 | 0,927 | -[c] | | -[c] | -[c] | -[c] |
| **8** | -751 ± 67 | 1.49 ± 0.30 | 0,52 ± 0,21 | 0,913 | -[c] | | -[c] | -[c] | -[c] |
| **9** | -1380 ± 109 | 2.74 ± 0.55 | 2,68 ± 0,44 | 0,895 | -[c] | | -[c] | -[c] | -[c] |
| **10** | -927 ± 71 | 1.84 ± 0.37 | 1,27 ± 0,27 | 0,909 | -[c] | | -[c] | -[c] | -[c] |

[a] iteratively determined following eq. 6 with $c_1 = 0$
[b] iteratively determined following eq. 8
[c] could not be determined

1. S. Radunz, H. R. Tschiche, D. Moldenhauer, U. Resch-Genger, *Sensors and Actuators B: Chemical* 2017, **251**, 490-494.